Pressure-induced Miscibility Increase of CH$_4$ in H$_2$O: A Computational Study Using Classical Potentials

Ciprian G. Pruteanu,[*,†,‡] Davide Marenduzzo,[*,†] and John S. Loveday[*,†]

†SUPA, School of Physics and Astronomy and Centre for Science at Extreme Conditions, The University of Edinburgh, Edinburgh EH9 3JZ, United Kingdom

‡Now at Department of Physics and Astronomy, University College London, Gower Street, London WC1E 6BT, United Kingdom

E-mail: cip.pruteanu@ucl.ac.uk; dmarendu@ph.ed.ac.uk; j.loveday@ed.ac.uk

Abstract

Methane and water demix under normal (ambient) pressure and temperature conditions, due to the polar nature of water and the apolar nature of methane. Recent experimental work has shown, though, that increasing the pressure to values between 1 and 2 GPa (10 to 20 kbar) leads to a marked increase of methane solubility in water, for temperatures which are well below the critical temperature for water. Here we perform molecular dynamics simulations based on classical force fields – which are well-used and have been validated at ambient conditions – for different values of pressure and temperature. We find the expected increase in miscibility for mixtures of methane and supercritical water; however our model fails to reproduce the experimentally observed increase in methane solubility at large pressures and below the critical temperature of water. This points to the need to develop more accurate force fields for methane and methane-water mixtures under pressure.

1

Introduction

Alkanes are saturated hydrocarbons which are found in crude oil.[1] Whilst they dissolve in organic solvents, they are insoluble in water under ambient temperature and pressure.[2] This is because of water's polarity, and because the network of hydrogen bonding in water is difficult to disrupt by molecules such as alkanes which only contribute van der Waals interactions to the solvent molecules.

The simplest alkane (and hydrocarbon) is methane, CH_4, which is also one of the simplest gases. Methane is important from a fundamental science perspective as it is a model system to study hydrophobic forces,[3] one of the most widespread intermolecular forces occurring in nature. The solubility of methane in water is important to a number of fields: for example, methane-water mixtures are found at the bottom of oceans,[4,5] and in the interior of planets (most notably Uranus, Neptune and Titan).[6]

At near-ambient and low pressures, the solubility of a gas like methane in water is well described by Henry's law, according to which the concentration of a gas in a liquid is proportional to its partial pressure. As the pressure increases, so does methane solubility, but only relatively weakly – for instance at 100° C and 0.2 GPa, it is still only 8×10^{-3} mol %.[7]

At much higher pressure, ab-initio molecular dynamics simulations[8] showed evidence of methane-water mixing, but at a temperature and pressure of 1800 K and 15 GPa, well above the critical point of water – which is found at 647 K and 20 MPa.[9] It was also hypothesised that a sufficiently large pressure can induce breaking of the H-bonds in water, and that this would lead to increase mixing of methane and water;[3] however structural studies of water show no evidence of the proposed H-bond breaking up to at least 6.5 GPa[10] so H-bond breaking effects on solubility, if they occur at all, would not be expected below this pressure.

In this context, recent experimental studies performed by Pruteanu et al[11] have revealed an unexpected effect of pressure on the miscibility of water-methane mixtures. It was found that in the range between 1 and 2 GPa, and at 100° C – well below the critical point of water – the solubility of methane exceeds 40 mol %. The mechanism underlying this striking

enhancement in mixing is currently not clear.

An obvious approach to elucidate the mechanism of the solubility is to carry out molecular dynamics simulations of the methane water system. There are well accepted force fields for both water and methane[12,13] which describe well the phase diagram of water[14] and the ambient conditions behaviour of methane.[15] Such approaches have been used to model behaviour of clathrate hydrates,[16–20] a problem which can be considered as the crystalline analogue of the mixing of fluids. Such approaches have also been successfully used in other related systems.[21] To quantify miscibility in simulations, we measured the entropy of mixing, which can be defined on the basis of information theory quantities (mutual information) as done in Brandani et al.[22] [1]. Whilst our simulations found that methane miscibility is strongly enhanced in supercritical water, as is expected thermodynamically,[23] they did not reproduce the experimental increase in mixing found for subcritical water under pressure found experimentally,[11] suggesting that new physics needs to be included in the existing classical force fields to explain that observation.

Methods

Our simulations of water-methane mixtures were all run by using the GROMACS[24] software. For water, we considered three different force fields: TIP3P, TIP4P[25] and SPCE;[26] all these led to similar conclusions, so most of the results below are shown for a single force field (TIP4P). For methane, we used the OPLS-AA force field,[27] which has been calibrated to reproduce the behaviour of this substance at near-ambient conditions.[15] As our goal is to see how these well-used potentials fare at different pressures, in our simulations we did not change any of the parameters except for T and p.

For all simulations involving a chosen water potential the same initial condition and box size were used. Molecule numbers were chosen as follows:

---

[1]As we are mostly interested in qualitatively determining whether mixing is enhanced or not by pressure, more extensive quantifications of mixing were not pursued here.

- 944 H_2O and 470 CH_4 molecules for TIP3P = 33.2% moles CH_4

- 961 H_2O and 470 CH_4 molecules for TIP4P = 32.8% moles CH_4

- 942 H_2O and 466 CH_4 molecules for SPCE = 33.1% moles CH_4

After the creation of the initial box having the desired concentration, an energy minimization was performed, followed by a 100 ps NVT (isochoric-isothermal) equilibration at the target temperature and subsequently a 100 ps NPT (isobaric-isothermal) equilibration at the desired pressure and temperature. Following these steps, the production runs were carried out for a total time of 20 ns using a 2 fs time step. For all runs, and for both water and methane molecules a Nose-Hoover thermostat[28,29] was used (typical time constant 1 ps), along with Parrinello-Rahman coupling for pressure[30] (typical time constant 5 ps). A 1.1 nm cut-off was used for non-bonded interactions along with the Particle Mesh Ewald method[31] for Coulomb interactions. Finally, the LINCS algorithm was used to ensure the geometrical integrity of molecules throughout all runs. A representative isotherm curve at 500K is shown in Fig. 1.
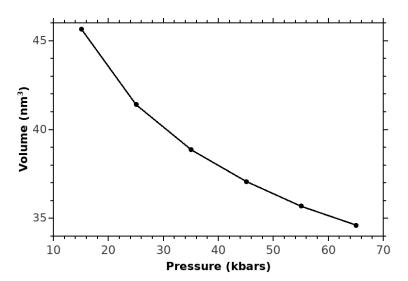

Figure 1: Equation of state for the simulation box used to study isothermal compression at 500K.

In what follows, as a basic probe of mixing we shall initially use radial distribution functions (RDFs) of different pairs of atoms – we shall focus on carbon-oxygen and oxygen-

hydrogen in water. It is important to highlight that RDFs in inhomogeneous systems need to be treated with care. These quantities are radially averaged, which is natural only for homogeneous systems. For phase separated systems, the density of, e.g., CH_4 is clearly inhomogeneous hence the distribution function involving atoms in this molecule is shifted up at small distances (as a molecule of a given species will have far more neighbours of its own kind than it would in a uniform mixture of the same concentration), and fail to tend to 1 for large distances. In order to determine changes in the coordination of certain pairs of atoms in the demixed systems, the peak height for each neighbouring shell therefore needs to be scaled to the value of the RDF at high distances, so they cannot be read directly from the plots.

Results and discussion

Most of our simulations were initialised with water and methane demixed (see Fig. 2), although simulations with mixed initial conditions gave indistinguishable results. We ran simulations corresponding to two ranges of pressure and temperature conditions. First, we considered a temperature range encompassing the critical point of water, to study the behaviour of a mixture of methane and supercritical water under pressure. Second, we considered a mixture of methane and non-supercritical liquid water (at 500 K), at a range of high pressures, up to values 3-fold higher than those experimentally found to promote methane miscibility in.[11] For both cases, we expect the initially phase separated mixture to mix. In the first case, this is due to the standard thermodynamic behaviour of mixtures at high temperatures;[23] in the second case, this expectation is based on the recent experiments in.[11] We now report our simulation results for these two sets of conditions separately.
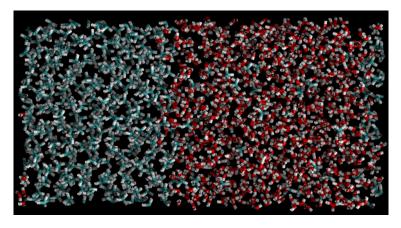
Figure 2: Snapshot of the simulation box at the beginning of the simulation, with methane and water fully demixed. Oxygen atoms are coloured red, carbon atoms turquoise and hydrogen atoms white.

Supercritical behaviour

We first analyzed the water-methane system for temperatures between 500 and 900 K, and at pressures of 15 kbar and 25 kbar. These two temperatures are respectively below and above the critical temperature of water.

To validate our simulations, we first computed the mean square displacements (MSDs) of water and methane molecules, for each condition. The MSDs are linear at all times, confirming that the simulated mixture remains in the fluid state for the entire duration of the production runs. Therefore the water system at 800 K is a supercritical fluid. As can be intuitively expected, the MSDs decrease with increasing pressure and decreasing temperature.

In order to quantify the state of the system – mixed or unmixed – we computed the partial radial distribution functions (RDFs) as well as the entropy of mixing as described in.[22] Hereafter we show results for TIP4P only, as the other two water potentials (TIP3P and SPCE) led to very similar results.
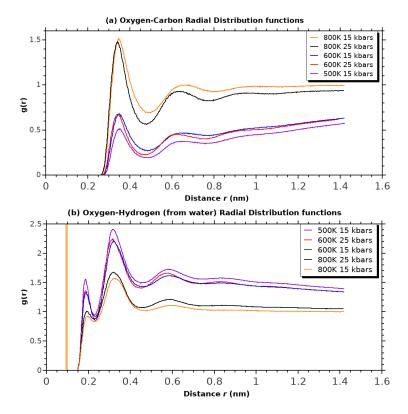
Figure 3: Selected radial distribution functions (RDFs) for (a) oxygen-carbon pairs and (b) oxygen - hydrogen (belonging to water) pairs at various pressures and temperatures.

The RDF plots show the main oxygen-carbon correlation function strongly increases with temperature, suggesting the two species mix. Figure 3 shows that the effect of pressure on mixing is minor, while temperature is the driving factor. Indeed, the RDFs at 800 K are similar for both the 15 kbar and the 25 kbar runs, and vastly different from the RDFs at 500 K and both pressures. As it can be seen in the oxygen – water hydrogen RDFs, the peak at ~ 0.18 nm, characteristic of hydrogen bonding, decreases drastically with increasing temperature. This is expected, as it is well known that once water goes through the critical point H-bonding disappears.[23,32] This means that water molecules cluster together less, therefore mixing more readily with the hydrophobic species (CH_4). We note in passing that this critical point is slightly below 600K – hence lower than in experiments – for TIP3P and TIP4P.[33]

The same conclusions can be drawn from the entropy of mixing (Fig. 4). The runs at 800 K are close to fully mixed – as the entropy of mixing is close to its maximum possible

value, which is 1 – while the ones at 500 K (below the critical temperature of water) are demixed, oscillating around the baseline value corresponding to a fully partitioned two-phase system having the overall composition of our system. In our simulations, the extent of mixing appears to increase smoothly with temperature.
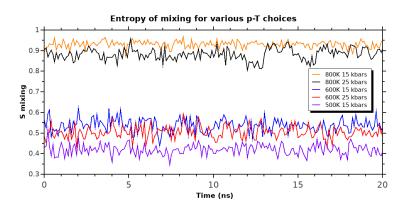

Figure 4: Plot of the entropy of mixing over time for methane-water mixtures at different pressures, for temperatures below and above the critical temperature for water.

High pressure non-supercritical behavior

In order to isolate the effect of pressure alone on the system and to attempt to reproduce the experimental results of,[11] we calculated an isotherm at 500 K and increasing pressure.

After performing the same analysis as in the case of supercritical water, we found that in this case all curves were qualitatively similar, so that no significant changes were observed due to pressure either in the RDFs or in the entropy of mixing (Fig. 5). The latter quantity actually shows a weak decrease with pressure. This decrease is also found at 600 K and 800 K, where it is more significant (Fig. 4). The weak decrease in mixing with increasing pressure may be explained by inspecting the RDFs in Fig. 3, which (especially at high temperatures) show an increase in the H-bonding peak of water, suggesting an increase in first-shell clustering of water molecules (which would reduce mixing).
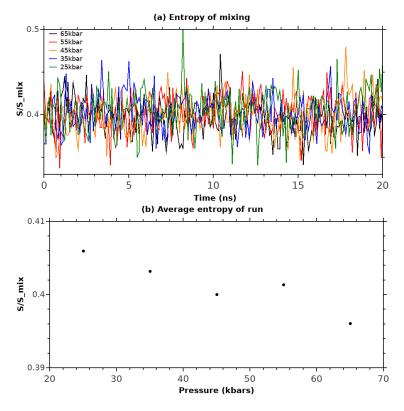
Figure 5: (a) Plot of the entropy of mixing over time, for simulations with subcritical liquid water and different values of the pressure (up to 60 kbar). (b) Average over time of the entropy of mixing as a function of pressure (for $T = 500$ K).

These results show that the potentials we used for methane and water predict demixing even under high pressure, thereby failing to reproduce the experimentally observed behaviour.

Potentials of mean force

To get more insight into our results, we revisited the potential of mean field (PMF) calculation between two methane molecules in water.[34] Here, we focused on higher pressure values, which are closer to those for which experiments observed methane-water mixing.[11] Other technical differences to keep in mind are that we considered two methane molecules instead of two methane-size cavities, and that we used TIP4P water instead of SPCE water, although we checked in selected cases that different force fields lead to qualitatively similar results.

The PMFs we obtained are shown in Figure 6a for a range of pressures and for a 500K (subcritical) temperature. The two first (and deepest) minima in the PMF correspond respectively to the two methane molecules being in contact (first minimum, or "contact minimum"), and to the two molecules being separated by a single water molecule (second minimum, or "solvent-separated minimum"). At ambient pressure, the contact minimum is much deeper than the solvent-separated medium, consistently with the fact that methane molecules aggregate and demix from water in the mixture.
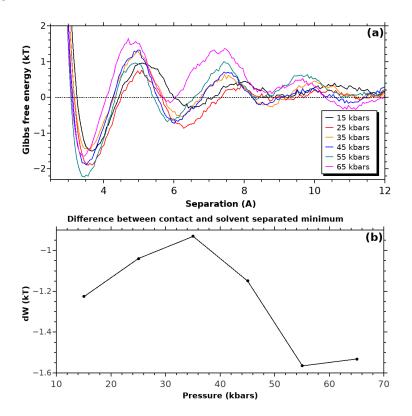

Figure 6: (a) Potential of mean forces for mixtures of methane and subcritical water, at different pressure. (b) Difference between the PMF values at the contact minimum and the solvent-separated minimum.

An increase in pressure initially leads to a decrease in the difference between the minima values, however for larger pressures this trend is reversed (Fig. 6b). Therefore, the minima difference changes non-monotonically with pressure; importantly, nowhere do we find the solvent-separated minimum to be the global one. These results are similar to those obtained (for lower pressures) in,[34] and are in line with our previous observations from direct molecular

10

dynamics simulations that demixing is never observed.

Conclusions

In summary, we have simulated here the phase behaviour of a methane-water mixture under high pressure and at different temperatures, both below and above the critical temperature of water. The potentials we used for both methane and water are well accepted, and have been shown to reproduce a number of experimental results for these systems. Our simulations correctly recreate temperature-induced mixing, when thermal fluctuations destroy the H-bond network in supercritical water. However, and more importantly, the potentials we used are unable to reproduce the pressure-induced mixing recently observed experimentally in mixtures with subcritical water. Our study also showed that H-bonding network is weakly affected by pressure in the latter regime, and that oxygen atoms maintain the typical tetrahedral coordination they have in pure water.

Our results therefore point to the need to improve classical force fields for methane and water mixtures under pressure. A possible avenue to do so would be to use ab-initio (e.g., Carr-Parrinello) molecular dynamics simulations, although the timescales and lengthscales which could be reached would be by necessity smaller than in our current study.

What underlies the dramatic pressure-induced increase in mixing, and why is this missed by our simulations? We can speculate about two possible mechanisms for mixing. First, there may be a subtle changes in water dipole moment and the H-bonding under pressure. The local environment is not electrically neutral and this may have a significant effect on the methane potentials. Second, pressure may change the relative molecular volumes of methane and water in such a way that then it becomes possible for methane to squeeze into an essentially unperturbed water H-bond network. Such behaviour is observed in the crystalline phases where the hydration number drops from $5.75 : 1$ near ambient pressure to $2 : 1$ at 2 GPa.[35] If either of this mechanisms is at work in the experiments, we hypothesise

that our current simulations are missing them either because the compressibility under high pressure of water and methane does not match the real-world values – similarly to what is observed for water compressibility at high T[36] – or because of polarisability effects in either methane or water, which are absent in the modelling. Whatever the mechanism of pressure-induced mixing, and the missing ingredient in the simulations, it would be interesting to pursue these questions further in the future.

Finally, we note that the methane potentials we are using are widely employed for modelling of clathrates and other related systems at pressure. The fact that they fail to reproduce behaviour as important as mixing at such low pressures has important consequences for other predictions made using these potentials.[16,21]

Acknowledgement

References

(1) Furniss, B. S. *Vogel's Textbook of Practical Organic Chemistry*; Pearson Education India, 1989.

(2) Hermann, R. B. Theory of Hydrophobic Bonding. II. Correlation of Hydrocarbon Solubility in Water with Solvent Cavity Surface Area. *J. Phys. Chem.* **1972**, *76*, 2754–2759.

(3) Chandler, D. Interfaces and the Driving Force of Hydrophobic Assembly. *Nature* **2005**, *437*, 640.

(4) Gornitz, V.; Fung, I. Potential Distribution of Methane Hydrates in the World's Oceans. *Global Biogeochem. Cycles* **1994**, *8*, 335–347.

(5) Kvenvolden, K. A. Methane Hydrate - a Major Reservoir of Carbon in the Shallow Geosphere? *Chem. Geol.* **1988**, *71*, 41–51.

(6) Lunine, J. I.; Stevenson, D. J. Clathrate and Ammonia Hydrates at High Pressure: Application to the Origin of Methane on Titan. *Icarus* **1987**, *70*, 61–77.

(7) Duan, Z.; Mao, S. A Thermodynamic Model for Calculating Methane Solubility, Density and Gas Phase Composition of Methane-bearing Aqueous Fluids from 273 to 523 K and from 1 to 2000 bar. *Geochim. Cosmochim. Acta* **2006**, *70*, 3369–3386.

(8) Lee, M.-S.; Scandolo, S. Mixtures of Planetary Ices at Extreme Conditions. *Nature Comm.* **2011**, *2*, 185.

(9) Steeper, R. R.; Rice, S. F.; Kennedy, I. M.; Aiken, J. D. Kinetics Measurements of Methane Oxidation in Supercritical Water. *J. Phys. Chem.* **1996**, *100*, 184–189.

(10) Strässle, T.; Saitta, A.; Le Godec, Y.; Hamel, G.; Klotz, S.; Loveday, J.; Nelmes, R. Structure of Dense Liquid Water by Neutron Scattering to 6.5 GPa and 670 K. *Phys. Rev. Lett.* **2006**, *96*, 067801.

(11) Pruteanu, C. G.; Ackland, G. J.; Poon, W. C.; Loveday, J. S. When Immiscible Becomes MiscibleMethane in Water at High Pressures. *Sci. Adv.* **2017**, *3*, e1700240.

(12) Sakamaki, R.; Sum, A. K.; Narumi, T.; Ohmura, R.; Yasuoka, K. Thermodynamic Properties of Methane/Water Interface Predicted by Molecular Dynamics Simulations. *J. Chem. Phys.* **2011**, *134*, 144702.

(13) Docherty, H.; Galindo, A.; Vega, C.; Sanz, E. A Potential Model for Methane in Water Describing Correctly the Solubility of the Gas and the Properties of the Methane Hydrate. *J. Chem. Phys.* **2006**, *125*, 074510.

(14) Sanz, E.; Vega, C.; Abascal, J.; MacDowell, L. Tracing the Phase Diagram of the Four-site Water Potential (TIP4P). *J. Chem. Phys.* **2004**, *121*, 1165–1166.

(15) Jorgensen, W. L.; Madura, J. D.; Swenson, C. J. Optimized Intermolecular Potential Functions for Liquid Hydrocarbons. *J. Am. Chem. Soc.* **1984**, *106*, 6638–6646.

(16) Alavi, S.; Ripmeester, J. A.; Klug, D. D. Molecular Dynamics Study of the Stability of Methane Structure H Clathrate Hydrates. *J. Chem. Phys.* **2007**, *126*.

(17) Tse, J. S. In *Reviews in Computational Chemistry, Vol 28*; Parrill, AL and Lipkowitz, KB,, Ed.; Rev. Comp. Chem.; 2015; Vol. 28; pp 315–389.

(18) English, N. J.; MacElroy, J. M. D. Perspectives on Molecular Simulation of Clathrate Hydrates: Progress, Prospects and Challenges. *Chem. Eng. Sci.* **2015**, *121*, 133–156.

(19) Hiratsuka, M.; Ohmura, R.; Sum, A. K.; Alavi, S.; Yasuoka, K. A Molecular Dynamics Study of Guest-Host Hydrogen Bonding in Alcohol Clathrate Hydrates. *Phys. Chem. Chem. Phys.* **2015**, *17*, 12639–12647.

(20) Ning, F. L.; Glavatskiy, K.; Ji, Z.; Kjelstrup, S.; Vlugt, T. J. H. Compressibility, Thermal Expansion Coefficient and Heat Capacity of CH4 and CO2 Hydrate Mixtures Using Molecular Dynamics Simulations. *Phys. Chem. Chem. Phys.* **2015**, *17*, 2869–2883.

(21) Saitta, A. M.; Datchi, F. Structure and Phase Diagram of High-Density Water: The Role of Interstitial Molecules. *Phys. Rev. E* **2003**, *67*, 020201.

(22) Brandani, G. B.; Schor, M.; MacPhee, C. E.; Grubmüller, H.; Zachariae, U.; Marenduzzo, D. Quantifying Disorder Through Conditional Entropy: an Application to Fluid Mixing. *PloS ONE* **2013**, *8*, e65617.

(23) Letcher, T. M. *Thermodynamics, Solubility and Environmental Issues*; Elsevier, 2007.

(24) Abraham, M. J.; Murtola, T.; Schulz, R.; Páll, S.; Smith, J. C.; Hess, B.; Lindahl, E. GROMACS: High Performance Molecular Simulations Through Multi-level Parallelism from Laptops to Supercomputers. *SoftwareX* **2015**, *1*, 19–25.

(25) Aragones, J. L.; Vega, C. Plastic Crystal Phases of Simple Water Models. *J. Chem. Phys.* **2009**, *130*, 244504.

(26) Berendsen, H. J. C.; Grigera, J. R.; Straatsma, T. P. The Missing Term in Effective Pair Potentials. *J. Phys. Chem.* **1987**, *91*, 6269–6271.

(27) Martin, M. G.; Siepmann, J. I. Transferable Potentials for Phase Equilibria. 1. United-Atom Description of n-Alkanes. *J. Phys. Chem. B* **1998**, *102*, 2569–2577.

(28) Hoover, W. G. Canonical dynamics: Equilibrium Phase-space Distributions. *Phys. Rev. A* **1985**, *31*, 1695–1697.

(29) Nose, S. A Unified Formulation of the Constant Temperature Molecular Dynamics Methods. *J. Chem. Phys.* **1984**, *81*, 511–519.

(30) Parrinello, M.; Rahman, A. Polymorphic Transitions in Single Crystals: A New Molecular Dynamics Method. *J. Appl. Phys.* **1981**, *52*, 7182–7190.

(31) Darden, T.; York, D.; Pedersen, L. Particle Mesh Ewald: An N log (N) Method for Ewald Sums in Large Systems. *J. Chem. Phys.* **1993**, *98*, 10089–10092.

(32) Soper, A. The Radial Distribution Functions of Water and Ice from 220 to 673 K and at Pressures up to 400 MPa. *Chem. Phys.* **2000**, *258*, 121–137.

(33) Vega, C.; Abascal, J. L. F.; Conde, M. M.; Aragones, J. L. What Ice Can Teach us about Water Interactions: a Critical Comparison of the Performance of Different Water Models. *Faraday Discuss.* **2009**, *141*, 251–276.

(34) Hummer, G.; Garde, S.; Garcia, A. E.; Paulaitis, M. E.; Pratt, L. R. The Pressure Dependence of Hydrophobic Interactions is Consistent with the Observed Pressure Denaturation of Proteins. *Proc. Natl. Acad. Sci. USA* **1998**, *95*, 1552–1555.

(35) Loveday, J.; Nelmes, R.; Guthrie, M.; Belmonte, S.; Allan, D.; Klug, D.; Tse, J.; Handa, Y. Stable Methane Hydrate above 2 GPa and the Source of Titan's Atmospheric Methane. *Nature* **2001**, *410*, 661.

(36) Vega, C.; Abascal, J. L. F. Simulating Water with Rigid Non-Polarizable Models: a General Perspective. *Phys. Chem. Chem. Phys.* **2011**, *13*, 19663–19688.

Graphical TOC Entry

Solution Phase Separating

Binary Mixtures of Methane and Water

Solution Undergoing Mixing